Proceedings of BALTTRIB'2022 edited by prof. J. Padgurskas
eISSN 2424-5089 (Online)

DOI: 10.15544/balttrib.2022.9

CHARACTERIZATION OF AN ANTI-WEAR COATING FOR THE APPLICATION OF HIGHLY LOADED SMART THIN-FILM SENSORS

D. Konopka [1]*, F. Pape [1], R. Ottermann [2], T. Steppeler [2], F. Dencker [2], M.C. Wurz [2], G. Poll [1]

[1] Institute of Machine Design and Tribology (IMKT), Leibniz Universität Hannover, Germany
[2] Institute of Micro Production Technology (IMPT), Leibniz Universität Hannover, Germany

Abstract. The global change in terms of economic and ecological requirements necessitates the application of innovative technologies. In addition, resources must be used more efficiently. Rolling bearings are still a part of almost all machines in industry to transmit rotational movements and mechanical loads. These systems, in addition to using high-strength and expensive materials, have higher requirements within manufacturing tolerances. Conventional machine elements in particular have optimization potential in terms of service life and reliability. To advance this potential, sensor integration for intelligent system monitoring combined with a compact electronic solution has to be realized. Technological progress in terms of digitization also makes it possible to handle large volumes of data and evaluate them in a targeted manner. Commercial applications for large rolling bearings are already available. The operating states are monitored via Condition Monitoring Systems (CMS). For this process, vibration sensors are used to identify bearing damage. Friction behavior can also be determined via additional temperature sensors. In this work, the tribological contact will be examined in more detail and sensor arrays will be applied inside the bearing system. This article presents the first stages of applying a thin-film sensor to the rolling bearing surface and analyzing it in terms of tribological loading. The thin-film sensor and the bearing surface were stressed in a defined manner by a microtribological tribometer. To protect the sensor from wear mechanisms, an aluminium oxide (Al_2O_3) thin film is deposited on the surface of the rolling bearing. After the tests, the wear track will be characterized. The focus of the investigation is the friction mechanisms and the adhesion strength. It was shown that the protective coating of the thin film sensor had an influence within the tribological system, but could be used under the given conditions.

Keywords. Bearings, Smart Thin-Film Sensors, Coating, Micro tribology, Friction, Wear.

1. INTRODUCTION

Over the past few years, technological improvements enable to make people and machines smarter. This trend is also observed in conventional machine elements such as the rolling bearings or gears. The primary aim is to save resources and to control and update machines wireless. At the same time, the focus is also on optimizing lubricants or tribological rolling contacts in order to minimize friction. In the German Research Foundation (DFG) Priority Program 2305 "Sensor-Integrating Machine Elements (SiME)" project, an attempt is being made to observe machine elements in operation over the longer term and to analyze the operating conditions. In case of temperature changes or increase of vibrations within the system, maintenance intervals shall be optimized and downtimes prevented. By investigating the elasto-plastic deformation of the material subsurface, the bearing raceway by integrating strain sensors on the surface, the condition of the bearing can be obtained. Especially in the case of large bearings used for wind farms, the ordering and process of delivery can take more than a year. The project aims to obtain information and the operating status of the system directly from the tribological contact. For this purpose, thin-film sensors with corresponding micro-controllers are to be integrated and used in bearing systems.

* Author for contacts: Denis Konopka
E–mail: konopka@imkt.uni-hannover.de

First experimental results were obtained by the IMKT with the corresponding sensor technology in the 1980s [1, 2]. Thin-film sensors were applied into rolling bearings by means of a sputtering process. The aim was to measure the contact pressure and temperature in the elasto hydrodynamic rolling contact (EHD) by using a capacitive measurement method. A twin-disc test stand and a setup for cylindrical roller bearings were used. This work was able to provide initial experimental results within direct rolling contact in a bearing with a thin-film sensor, and compared with the theoretical approaches of Dowson and Higginson of the EHD theory [3]. However, this measurement method was not developed for the continuous monitoring of operating conditions. In general, CMS systems are used for machine elements to continuously measure the operating states. Sensors are usually mounted outside of gearboxes and receive the required information (e.g. temperature gradients of lubricant) with a time delay.

This project focuses on a measuring system, which is to be integrated in the rolling contact on the bearings raceway and continuously record data. For example, Gao et al. presented a first concept of integrated sensor systems in the rolling contact with the aim of obtaining the operating conditions. The sensors used (piezo sensors) were able to measure tribological information (e.g. contact pressure, vibration) and communicate in real-time with a measuring computer [4]. This concept was developed for helicopters and serves as inspiration for the first smart rolling bearing systems.

For the investigations, a thin-film array sensor system is to be designed and applied directly on the raceway of a rolling bearing. The array consists of different sensors (three strain gauges and one temperature sensor). This design is intended, for example, to measure tangential stresses, material deformation and contact temperatures on the surface. In perspective, it should be possible to determine the lubricating conditions.

For the first tests, a thrust cylindrical roller bearing is used as the reference bearing. The selected system has the advantage that the surfaces have a plane/flat geometry. Figure 1 shows the components of the bearing. Secondly, the planned layer system is shown schematically on the right side. A first step is to apply the coating system on the surface of the housing washer. The coating is a multilayer system. Aluminum oxide (Al_2O_3) is used for electrical insulation. The temperature sensor is made of platinum (Pt) and the strain gauges are made of constantan ($Cu_{54}Ni_{45}Mn_1$). Finally, Al_2O_3 is applied on the surface as a top layer for additional insulation, but also against tribological abrasion. The entire multilayer system is realized with a PVD sputtering process. First thin films have already been deposited and investigated on steel samples for pre-investigations [4, 5]. Temperature-dependent changes and effects of ageing of strain gauges were investigated [4]. It has been shown that the deposited thin-film sensors performed well on the selected substrate. However, the results must now be transferred to rolling bearing surfaces. In contrast to the laboratory samples, these have a higher surface roughness.

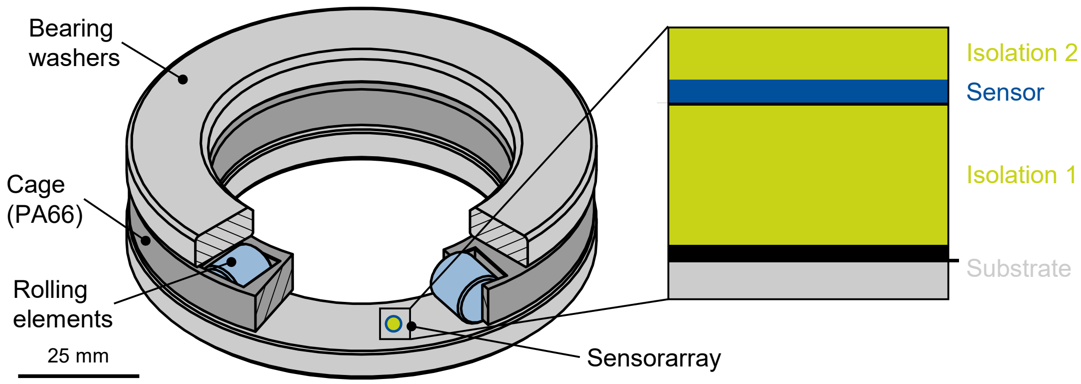

Figure 1. Illustration of the planned tribological system (cylindrical roller thrust bearing 81212) and an unscaled schematic illustration of the thin-film sensor layer system.

The aim of this study is to qualify an insulation layer on a hardened rolling bearing washer sufficient for the harsh conditions in cyclic rolling contacts with slip due to the contact conditions. The investigation is carried out from a tribological point of view. Higher roughness could negatively influence the adhesive strength. The roughness of the substrate has also a significant influence on the insulation layer.

It was shown in a previous investigation that a low roughness (Ra,max = 0.10 µm) has better electrical properties and the ohmic resistance decreases significantly when substrate roughness is increased [5]. Furthermore, the coatings have to resist tribological stresses. For this purpose, sliding tests are carried out on a tribometer. On the one hand, the coatings have the function of separating the sensor material (Pt and Const) from the substrate and, at the same time, providing wear protection.

Typical protective coatings can be made of Diamond like Carbon (DLC), Silicon nitride (Si_3N_4) or Al_2O_3. DLC coatings feature low coefficient of friction and as multilayer systems favorable tribological wear resistance [7]. But due to the electrical conductivity they cannot be used as insulating layers. Si_3N_4 features also good surface protection and can be deposited in a Plasma Enhanced Vapour Deposition process (PECVD) [8, 9]. For a sputter deposition process applying a target to generate the coating ceramic Al_2O_3 as hard protective coating lends itself for application.

Additional boundary conditions must be taken into account in the development and design of the wear coatings. The coating thicknesses may not be chosen arbitrarily high because, on the one hand, residual stresses of the coating material are induced if the coatings are too high. The residual stresses of the sputtered coatings could induce delamination [10, 11]. However, thicker Al_2O_3 coatings improve the insulation efficiency. In parallel, thicker top-layer coatings have the effect that the wear protection can have a longer service life.

2. EXPERIMENTAL

2.1. Preparation of Samples

The Al_2O_3 coatings investigated in the present study were deposited in an industrial PVD system (*Senvac Z550*). The coating itself is deposited on a steel substrate. A commercially available thrust bearing washer (*Schaeffler INA, Germany*) has been used as the substrate. The bearing washer is made of 100Cr6 (AISI 52500) and features a hardness of about *60 HRC*. Before the substrate is inserted into the coating system, the surfaces must be cleaned. To protect against corrosion on the surface, a conservation liquid is applied by the manufacturer, which must be removed in a first step. Furthermore, surfaces must be oil-free with a view to providing good adhesion. Therefore, the surfaces are cleaned in an ultrasonic bath for 10 min in ethanol and for another 10 min in isopropanol thoroughly. After the cleaning process, the samples are positioned in the recipients located under the sputtering target. The distance between the Al_2O_3 target and the substrate was about 100 mm. Before the coating process can be started, the vacuum chamber has to be evacuated. The PVD sputtering process is carried out under a high vacuum. If the base pressure of $1 \cdot 10^{-5}$ mbar is reached, a coating with sufficient insulation and adhesion properties can be achieved. To improve the adhesive bonding, the surface is treated again by Argon plasma etching before coating. This step removed material from the surface for a few nm. This removal is minor, that it has no effect on the surface roughness or the general structure of the surface layer (results shown later will prove this). For plasma etching, the sputter power was set to 200 W and the pressure was set to $3.1 \cdot 10^{-3}$ mbar. The bias voltage was 85 V and argon (Ar) was used as the inert gas. The process step was set to 10 min. Immediately after cleaning, the sputter deposition was started without breaking the vacuum. The sputtering power was increased to 400 W for the Al_2O_3 layer. Due to corresponding preliminary investigations of the insulation layer, different coating thicknesses were selected for this investigation by means of a known deposition rate of 8.3 nm/min and thus the process time was varied. For an overview of the process parameters and the prepared samples, see Table 1.

Table 1. Overview of PVD parameter

Plasma etching	Pressure	$3.1 \cdot 10^{-3}$	mbar
	Power	200	W
	Duration	10	min
Sputtering	Pressure	$3.1 \cdot 10^{-3}$	mbar
	Power	400	W
	Bias	85	V
	Target material	Al_2O_3	-
	Sputter gas	Ar	-
	Deposition rate	8.3	nm/min

Table 2. Description of prepared samples

	Sample 1	Sample 2	Sample 3	Reference	
Layer thickness	2	4	6	0	µm
Sputter duration	240	480	960	0	min

2.2. Analytic

Surfaces of the samples used were analyzed before and after the coating process and tribological tests. A VK-X250K laser scanning microscope (Keyence Deutschland GmbH, Germany) was used for this purpose. For the evaluation of the tests, various 3D images are created along the scratches or movement paths performed in the Milli-Tribometer and Scratch Tester (TriboTechnic, France). In addition, the surface profile was measured tactilely by using a perthometer (Mahr GmbH, Germany) with a diamond tip with a radius of 5 µm to gain information about the roughness. The roughness properties can change depending on the layer thickness. However, it is assumed that the sputtered surface structures are adopted by the substrate.

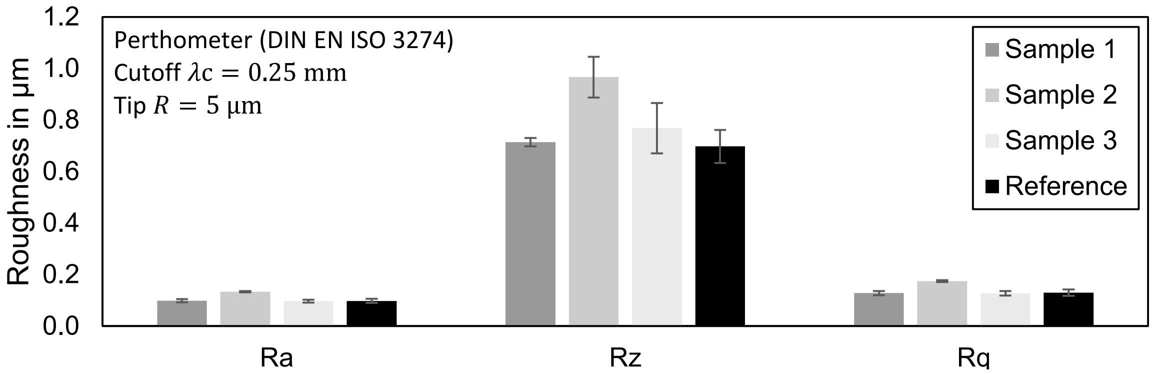

Figure 2. Determined roughness parameters (Ra, Rz and Rq) of the samples tested. A perthometer (Mahr GmbH) with a tip radius of 5 µm was used.

2.3. Wear-Tests

A microtribological tribometer (TriboTechnic, France) was used for the studies on the prepared coatings. On the one hand, the tribometer can investigate the influence of oil, metal working fluid and grease on friction at defined loads and relative speeds, and on the other hand it is used for the development of dry lubricant systems and thin films. The advantage is that quantitative and qualitative results can be generated under reproducible experimental conditions. The test setup consists of a specimen holder, the specimen and a counterbody (see Fig. 3). At the counterbody holder, the tangential force is detected by means of a displacement sensor and communicated to the measuring computer for further processing. The tangential force is a result of the defined relative movement between specimen and counterbody. Different geometries can be used as counterbody elements. However, the results of this study will be carried over to rolling bearings in perspective, so hardened steel balls of AISI 52500 and a diameter of Ø6 mm were used for this study. This material is also used in commercial rolling bearing components with similar material properties. By determining the tangential force, the coefficient of friction (CoF) is calculated. The lubricant used is a GLEITMO 585 K (Fuchs Lubricants GmbH, Germany) grease. For an overview of the test parameters, see Table 3.

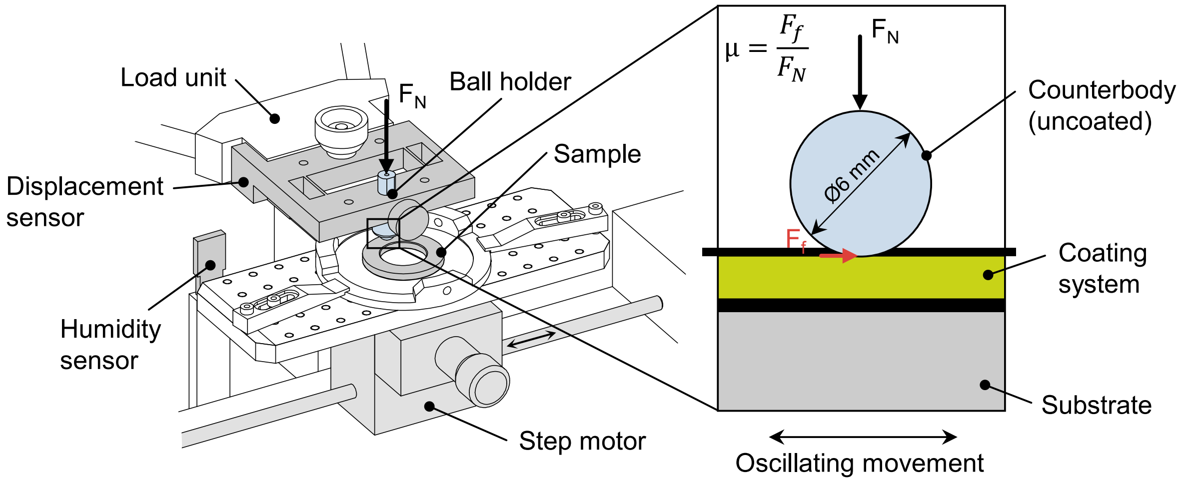

Figure 3. Experimental setup of the used tribometer (left) and a schematic illustration (right) of the tribological sliding contact (unscaled).

Table 3. Description of the experiments.

Sliding velocity	8			mm/s
Normal load	1	2	3	N
Hertzian pressure	660	830	950	MPa
Duration	208			min
Lubricant	Lithium based Gleitmo 585 K / NLGI 2 (Fuchs)			
Stroke	4			mm
Distance	100			m

From a tribological point of view, it is still important to mention that for the wear tests, moderate stresses were selected with regard to the normal force. However, because the ball is fixed in the specimen holder, pure sliding and high frictional energy can be expected in the tribological contact. In order to compare the efficiency of the wear protection coating Al_2O_3, the tests of the manufactured specimens are compared with reference specimens without any coating. An untreated axial bearing washer is used as a reference.

3. RESULTS & DISCUSSION

3.1. Sliding test with grease

The following describes the wear tests. All tests have been carried out under constant ambient conditions. At the same time, it has been ensured that the same amount of grease is distributed on the sample. An additionally designed dosage unit was used to ensure a constant quantity of grease for the wear track. However, when executing the test, it should be mentioned that due to the oscillating movements on the position set, the grease is pressed to the side and can only partially and undefined return back to the tribological contact. Because temperature also has a significant effect on the structure and viscosity of the grease, the temperature and humidity were kept approximately constant within the experimental series. The ambient temperature was 25 ± 1 °C. The relative humidity was 29 ± 6 %. It is necessary to mention that the tests were carried out over a longer period of time and therefore minimal variations occurred. The statistically determined variations within the tests can therefore be classified as acceptable.

Figure 4 shows a summary of all the tests carried out. As already described, three different normal loads were selected to stress the manufactured specimens. The results can be found on the horizontal axis in three categories. The added value in the parentheses describes the maximum Hertzian pressure taking into account the material characteristics of the tribological contact partners used.

First of all, the tests were carried out with 1 N load, respectively 660 MPa. For all three Al_2O_3 samples, it was noticeable that there was no significant increase over time for the coefficient of friction. At the same time, the reference sample was used for comparison and similar friction values were measured. The additional examination of the load steps 2 N (830 MPa) and 3 N (950 MPa) also showed no significant changes in the coefficients of friction during the test.

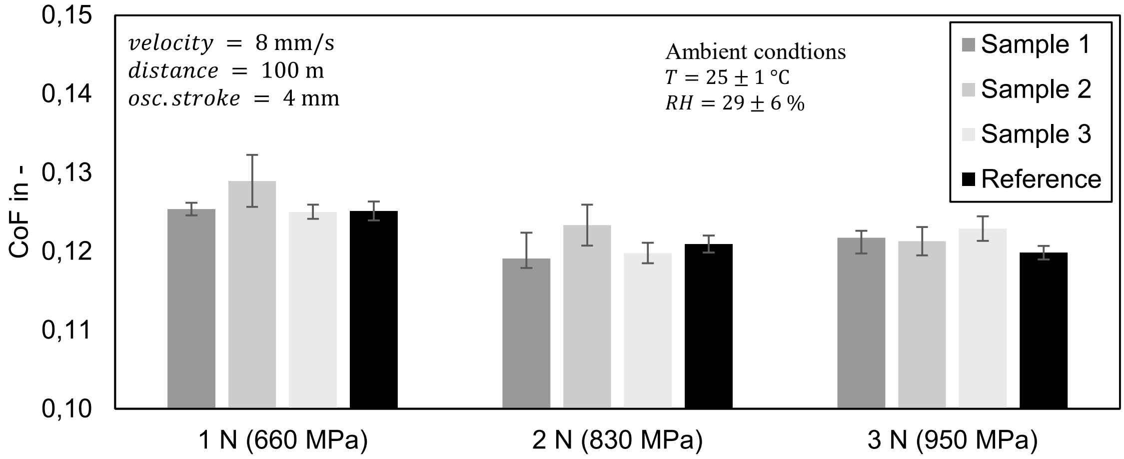

Figure 4. Overview of the CoF of all tests with grease in relation to the different loads.

A lower friction coefficient was observed on closer examination within the test series 2 N and 3 N. The reason for this could be that the excess grease must first be pressed out of the contact. This could generate a low resistance in the movement. In general, however, it can be determined for the grease-lubricated specimens and the reference that the layer thicknesses of the various specimens have no influence on the coefficient of friction. Also, the variation of the selected stress ranges between 660 MPa and 950 MPa had no influence on an increase of the friction coefficient. The tests could be repeated reproducibly and in a statically validated range. As an example, Figure 5 shows the time course of the different specimens with constant normal force (3 N) and relative velocity (8 mm/s). It can also be noted that the different coating thicknesses have not shown any negative influence on the measurement of the coefficient of friction. After the tests, the individual wear paths have been examined in the laser scanning microscope. The aim was to determine characterization criteria and differences between the individual tests. The focus was on delamination effects and wear differences.

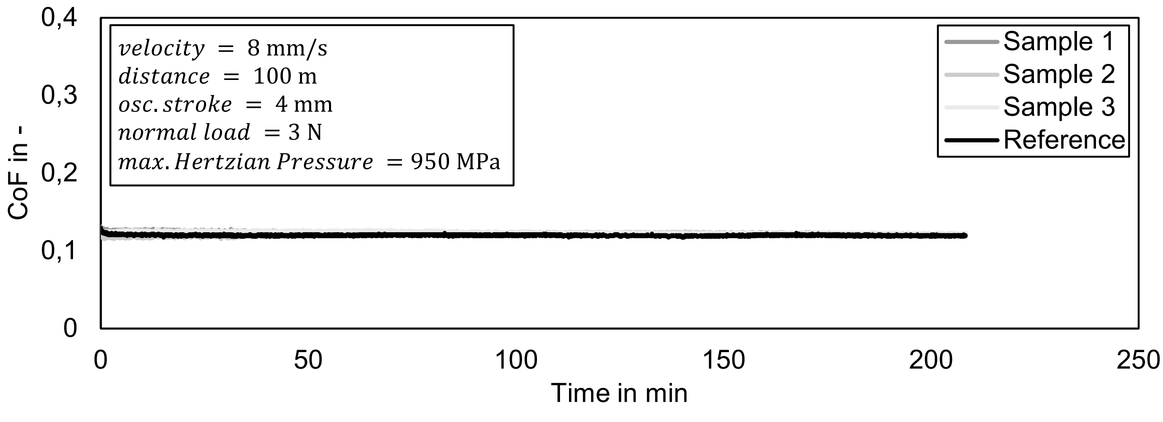

Figure 5. Time curve of the CoF from the test with grease and 3 N as normal force.

3.2. Sliding tests under dry solid contact

Although the conditions on the surfaces were very harsh (pure sliding), no macroscopic wear was observed in the sliding test and the prepared coatings showed a similar response in relation to the reference tests in the tribological system. The wear tracks on the axial washers and the surfaces of the balls used were investigated. For this reason, the tests were subsequently extended and repeated now without lubricant. The setup choice allowed solid contact and increased friction and wear behavior. The experimental parameters were adjusted the same except for the number of cycles. The test time was now only about 8 min instead of 200 min, so 500 cycles resulted. Figure 6 (a-c) shows the results of the dry sliding test. The diagrams in the figure show the time course of the different loads in each case. In a direct comparison of all tests, an initial value of the coefficient of friction of about 0.1 can be seen. In all tests, an increasing CoF can be seen after a short time. It can be assumed that although the surfaces are cleaned with isopropanol and there is no lubricant between the two contact partners, there has been a lubricating removal from an absorption layer. Particularly in the reference test (black curve), it is noticeable that the absorption layer is worn out after a few cycles. After that, an almost constant coefficient of friction of 0.7 is achieved. This coefficient of friction is typical for an abrasive wear with a steel-steel tribo-contact. A significant increase of CoF is also observed in the tests for Sample 1 (Al_2O_3, 2 µm) and Sample 2 (Al_2O_3, 4 µm). However, this occurs with a time offset and increases linearly and more smoothly.

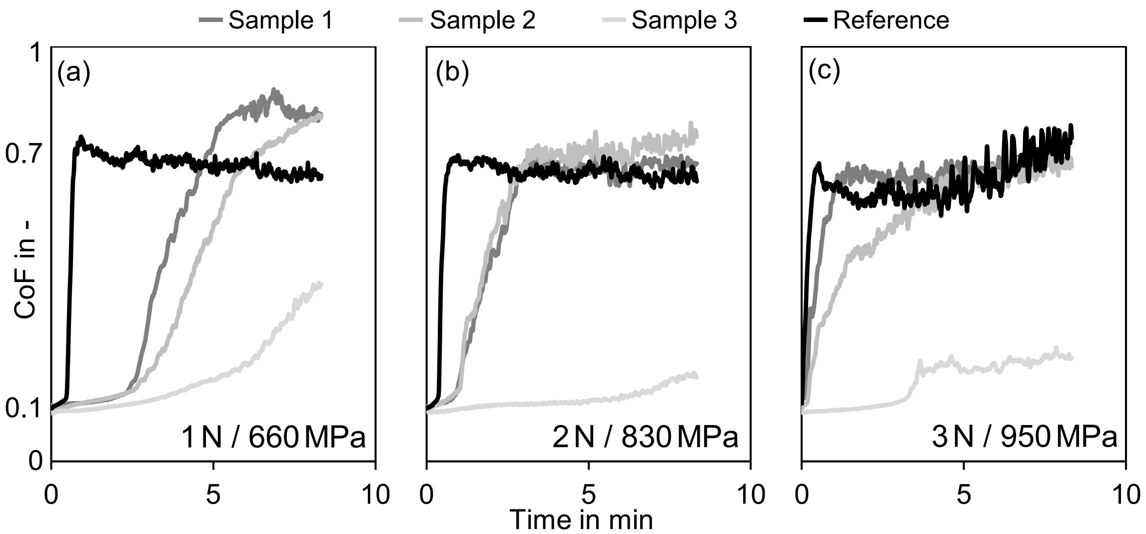

Figure 6. Results from the dry sliding tests with different load steps. (a) Normal load 1 N (p_{Hertz} = 660 MPa). (b) Normal load 2 N (p_{Hertz} = 830 MPa). (c) Normal load 3 N (p_{Hertz} = 950 MPa).

Only in Sample 3 with a coating thickness of 6 µm, a lubricating reaction is observed. At all three load steps, the CoF value of 0.7 is not reached. This shows that the tribological system has a lower affinity to abrasion on the one hand, and on the other hand reduces friction in the solid contact.

3.3. Damage analysis and discussion

After the experiments, optical microscope and laser scanning microscope were used to examine the wear tracks on the specimens. Furthermore, the applied steel balls were analyzed. The damage analyses of test with 3 N are presented as an example in Fig. 7. These are the sliding tests with a normal force of 3 N respectively a maximum Hertzian pressure of about 1 GPa.

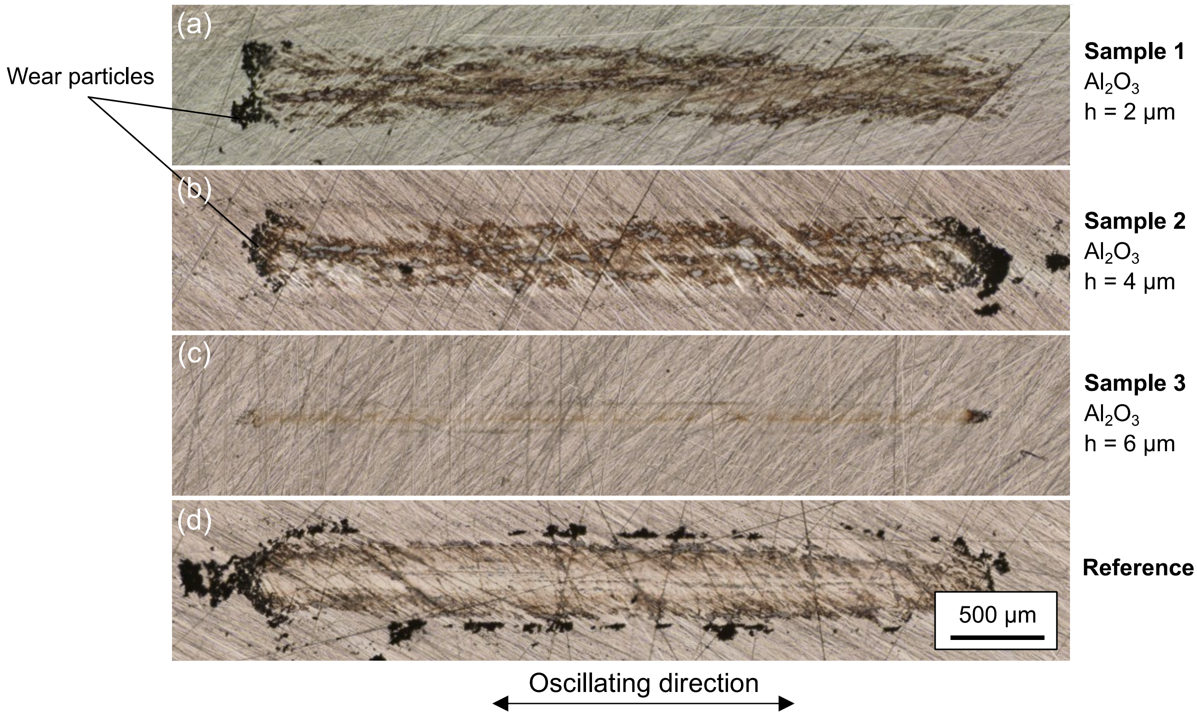

Figure 7. Wear tracks of the dry tests with 3 N (p_{Hertz} = 950 MPa) as normal load.

The wear tracks of the various tests can be clearly seen. With the exception of the microscopic image of Sample 3 (see Fig. 7 (c)), a considerable number of wear particles have been worn away from the contact zone in addition to the reddish formation of an oxide layer. A detailed examination of the wear tracks shows that the individual coating systems (Fig. 7 a-c) macroscopically still have the roughness from the initial state. In the case of the reference sample itself, in addition to the wear particles at the end of the wear track, there are also some distributed around the entire track. It can be assumed that the wear was highest here and the tribological stress, as shown in the sliding test results, occurred directly after the start of the test. At the same time, considerably more roughness peaks have already been worn away within the wear tracks than in relation to the coated samples. For this reason, the used balls from the dry test were still examined after the test. Figure 8 shows an example of the surface of the sphere of the experiment with Sample 3 and the reference sample. The inserted double arrow shows the direction of movement.

Figure 8 shows that the wear protection layer Al_2O_3 on the bearing washer reduces abrasion and is even lubricating in some cases. This was also proven by the coefficient of friction measurements. The corresponding analyses were carried out for each ball. It can be clearly seen that there is a correlation of the wear track from Figure 7 and the worn balls. The results are shown again graphically in Fig. 9. The wear tracks and the balls used from the dry test were measured and compared. Sample 3 is particularly outstanding in this context. In addition to the very small amount of wear, the friction values in the respective tests are also very low.

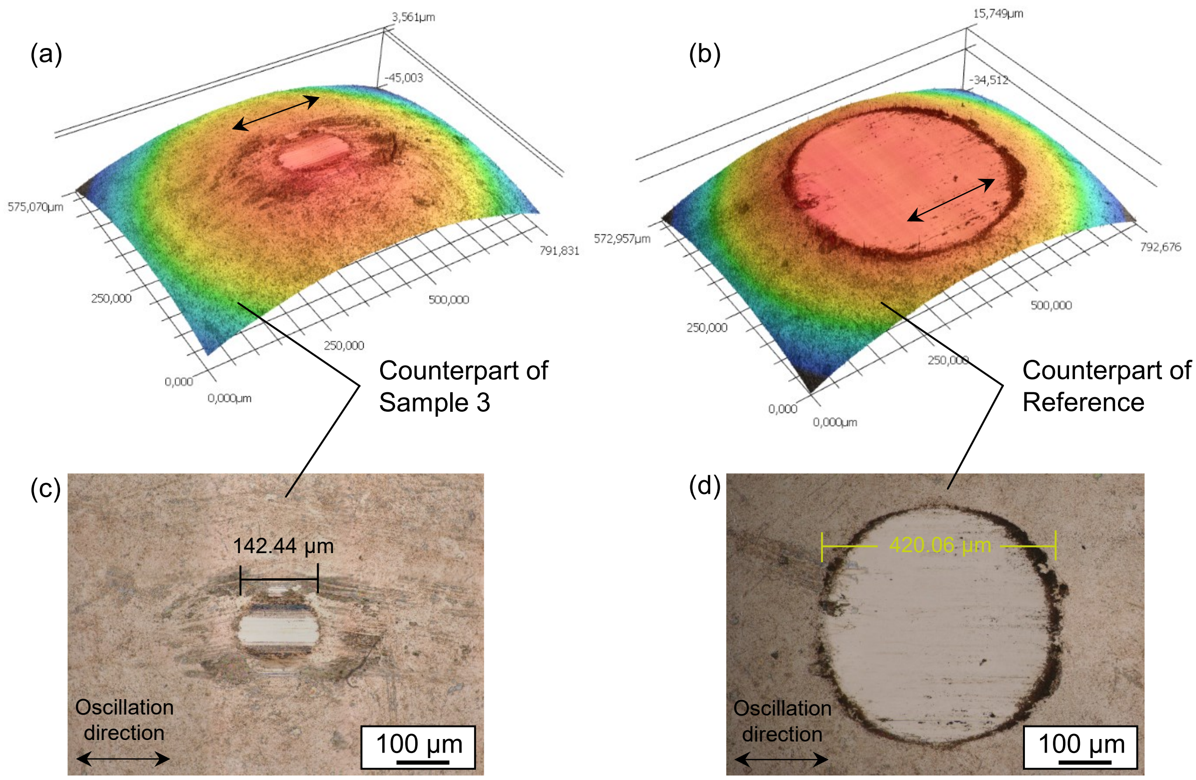

Figure 8. Laser microscope images of the surface of steel balls after the dry sliding test with 3 N. (a) Counterpart from the experiment with Sample 3 (Al_2O_3). (b) Counterpart from the reference test with significantly more wear in contrast to (a, c). (c-d) Top view of the balls with measurement of wear.

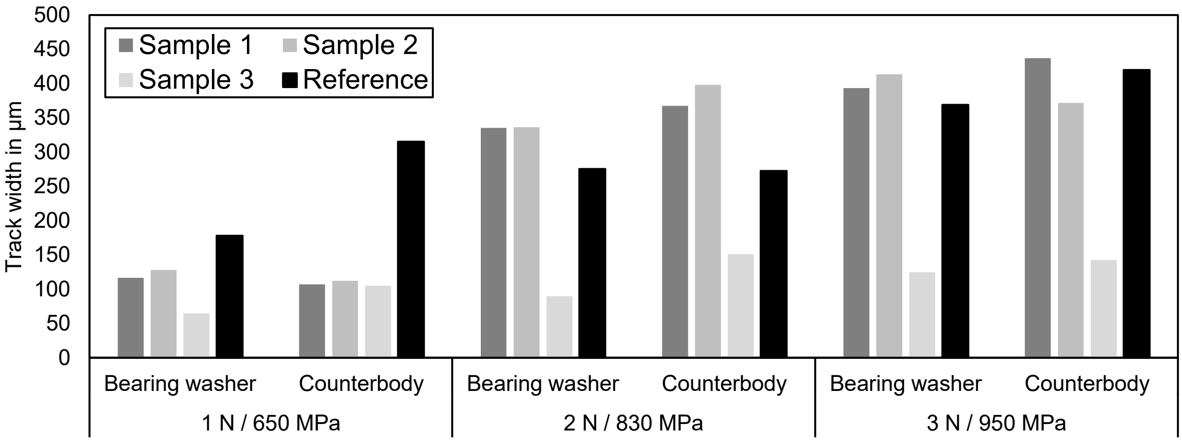

Figure 9. Overview of the wear track widths of the axial bearing washers and the steel ball used.

4. CONCLUSION

In the presented study, a variation of aluminum oxide coatings was successfully characterized and tested by tribological investigations. The focus was particularly on wear behavior and adhesion. The rolling bearing, which has an increased roughness, was chosen as the object of investigation. However, the coating system was successfully deposited on the surface with sufficient adhesive strength. The deposited Al_2O_3 was homogeneous and without defects (e.g. significant porosity). In particular, the tribological tests in dry contact did not produce any delamination or spalling. At the same time, the wear was significantly lower on the bearing washer itself, suggesting that the surfaces of the Al_2O_3 were harder than the significantly worn steel balls in the pin-on-plane test. Subsequently, it can be summarized that the deposited Al_2O_3 films had very good adhesive strength and performed very well in the sliding test with higher Hertzian pressures. Especially the material properties are interesting for further investigations. Therefore, the hardness and elasticity of the Al_2O_3 will be investigated with a nanoindenter in the next step. These data are also important for a planned contact mechanical simulation.

Furthermore, the sliding tests are extended on multilayer coatings. The present work dealt with the first project step generally: development and characterization of the insulation and wear protection layer. In the perspective, however, thin-film sensor materials such as Constantan and Pt (see Fig. 1) are to be deposited onto the bearing surface in interaction with Al_2O_3. A first design has already been successfully applied to a bearing washer (see Fig. 10).

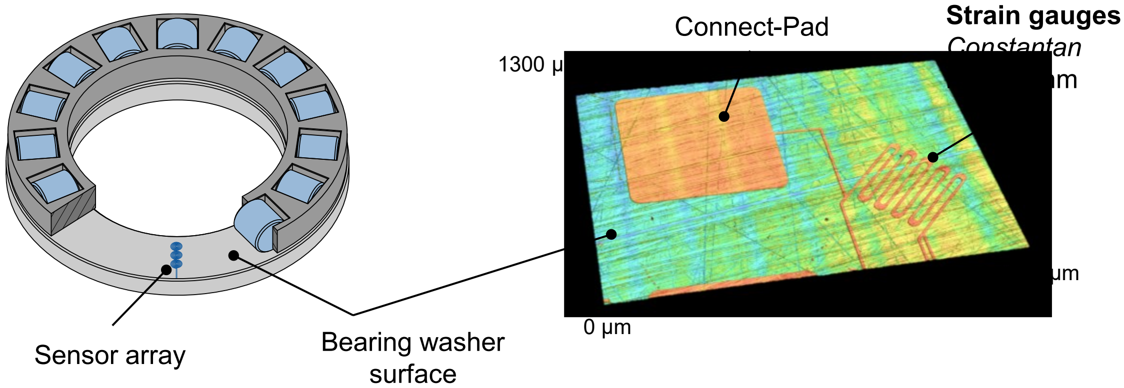

Figure 10. First trial of the sensor element of an array applied on a real geometry (cylindrical roller thrust bearings 81102). The strain gauge is made of Constantan ($Cu_{54}Ni_{45}Mn_1$) and has a thickness of 200 nm.

The thick coatings in particular were important for good insulation efficiency for the sensor manufacturer. It could be shown that exactly these coating systems (Sample 3 with coating thickness of 6 µm) also worked very well in tribological contact.

ACKNOWLEDGEMENTS

The results presented in this paper were obtained within the Priority Program 2305 "Sensor-Integrating Machine Elements (SiME)" (project number 441853410) in the subproject "Integrierte Sensorik für intelligente Großwälzlager (ISiG)" (Integrated Sensors for intelligent Large-Diameter Bearings) (project number 466778958). The authors would like to thank the German Research Foundation (DFG) for the financial and organizational support of this project.

REFERENCES

[1] Schmidt U. Die Schmierfilmbildung in elastohydrodynamischen Wälzkontakten unter Berücksichtigung der Oberflächenrauheit. Thesis, Leibniz University Hanover, 1985.
[2] Bauerochs R. Druck- und Temperaturmessungen in EHD - Wälzkontakten, Thesis, Leibniz University Hanover, 1989.
[3] Dowson D., Higginson G. R. Elastohydrodynamic lubrication - the fundamentals of roller and gear lubrication, The Commonwealth and International Library, Pergamon Press, London, 1966.
[4] Gao R., Holm-Hansen B., Wang C. Design of a mechatronic bearing through sensor integration. Proc. SPIE 3518, Sensors and Controls for Intelligent Machining, Agile Manufacturing, and Mechatronics, 1998, doi: 10.1117/12.332801.
[5] Ottermann R., et al., Direct Deposition of Thin-Film Strain Gauges with a New Coating System for Elevated Temperatures. 2020 IEEE SENSORS, pp. 1-4, 2020, doi: 10.1109/SENSORS47125.2020.9278661.
[6] Heikebrügge S., Ottermann R., Breidenstein B., et al. Residual Stresses from Incremental Hole Drilling Using Directly Deposited Thin Film Strain Gauges. Experimental Mechanics 62, pp. 701–713, 2022, doi: 10.1007/s11340-022-00822-0.
[7] Paulkowski D., Bandorf R., Achilles S., Pape F., Gatzen H.H., Bräuer G. Studies on Diamond-like Carbon Coatings for the Application in Micro Actuators, EUROMAT 2007 (accepted for Advanced Engineering Materials), Wiley-VCH Verlag Nuremberg, Germany, 2008.

[8] Pape F., Cvetkovic S., Kiesow A., Kailer A., Rissing L. Microtribological Evaluation of Unlubricated Sliding Bearings with Thin Si3N4 and PTFE Coatings, 18th Int. Conf. Wear of Materials. 3rd European Conf. on Tribology (ECOTRIB2011), Vienna, Austria, Vol. 2 (2011), pp. 747-752.
[9] Ruffert C., Pape F., Rissing L. Investigations on Silicon Nitride Thin Films Deposited by PECVD. European Congress and Exhibition on Advanced Materials and Processes (Euromat 2011), Montpellier, France, 2011.
[10] Teixeira V. Residual stress and cracking in thin PVD coatings. Vacuum, Volume 64, Issues 3–4, 2002, pp. 393-399, doi: 10.1016/S0042-207X(01)00327-X.
[11] Soni Sumit, et al. Residual Stress Mechanisms in Aluminium Oxide Films Grown by MOCVD, ECS Transactions, Volume 25, Number 8, 2009, doi:10.1149/1.3207737.